Phytochemistry 155 (2018) 126–135

Contents lists available at ScienceDirect

Phytochemistry

journal homepage: www.elsevier.com/locate/phytochem

Chemical and genomic diversity of six *Lonicera* species occurring in Korea

Kyo Bin Kang[a,1,*], Shin-Jae Kang[b], Mi Song Kim[a], Dong Young Lee[a], Sang Il Han[c], Tae Bum Kim[a], Jee Young Park[b], Jinwoong Kim[a,c], Tae-Jin Yang[b,**], Sang Hyun Sung[a,2]

[a] College of Pharmacy and Research Institute of Pharmaceutical Sciences, Seoul National University, Seoul, 08826, Republic of Korea
[b] Department of Plant Science, Plant Genomics and Breeding Institute, Research Institute of Agriculture and Life Sciences, College of Agriculture and Life Sciences, Seoul National University, Seoul, 08826, Republic of Korea
[c] Medicinal Plant Garden, College of Pharmacy, Seoul National University, Koyang, 12045, Republic of Korea

ARTICLE INFO

Keywords:
Lonicera
Caprifoliaceae
Chemical diversity
Genomic diversity
Chloroplast DNA
Specialized metabolites
LC–MS

ABSTRACT

Lonicera spp. (Caprifoliaceae) are important not only as a common medicinal herb in East Asia but also as one of the most problematic invasive species in North America. In the present study, we performed a systemic analysis of genomic and chemical diversity among six *Lonicera* species occurring in Korea, *L. japonica*, *L. maackii*, *L. insularis*, *L. sachalinensis*, *L. praeflorens*, and *L. vesicaria*, using chloroplast DNA whole genome shotgun (WGS) sequencing and LC–MS analyses. The phylogenetic and phylochemical relationships did not coincide with each other, but partial consistency could be found among them. InDel-based cDNA marker for authentication was developed based on the genome sequences. Flavonoids, iridoids, and organic acids were identified in the LC–MS analyses, and their inter-species distribution and localization were also revealed.

1. Introduction

The genus *Lonicera* (Caprifoliaceae; commonly known as honeysuckles) comprises approximately 180 species of arching shrubs or twining bines distributed throughout the northern hemisphere. Taxonomy and phylogeny within *Lonicera* has been extensively evaluated; since Rehder published a synopsis about a classification system for *Lonicera* species (Rehder, 1903), his system has been generally adopted by most botanists with only minor modifications (Hara, 1983; Hsu and Wang, 1988). In Rehder's system, *Lonicera* species are classified into two subgenera, *Lonicera* (with ca. 155 species) and *Caprifolium* (with ca. 25 species), and each subgenus is further categorized into four sections and numerous subsections. In 2008, the first study on the phylogenetic relationships among 47 *Lonicera* species was published based on the DNA sequences of the internal transcribed spacer (ITS) region of nuclear ribosomal DNA (nrDNA) and five chloroplast non-coding regions (Theis et al., 2008). Several studies further revealed the phylogeny among *Lonicera* species (Naugzemys et al., 2014; Smith, 2009; Smith and Donoghue, 2010), but most parts of the genomic diversity among many *Lonicera* species still remain uncharted.

A number of *Lonicera* species have been used in East Asian traditional medicines. The flower bud of *L. japonica* Thunb. is the most representative case, and it is the one of the most commonly used medicinal herbs for inflammation relief in traditional Chinese medicine (Shang et al., 2011). More than 200 compounds including flavonoids, organic acids, and iridoids have been isolated from *L. japonica* and other *Lonicera* species (Shang et al., 2011; Wang et al., 2016), and they exhibit various pharmacological effects such as antioxidative (Choi et al., 2007), anti-inflammatory (Lee et al., 1995), antiviral (Ding et al., 2017), and hepatoprotective (Sun et al., 2010) activities. However, in North America, some *Lonicera* species, such as *L. japonica*, *L. maackii* Rupr., *L. morrowii* Gray, *L. tatarica* L., and their hybrid *L.* × *bella* Zabel, have been identified as some of the most problematic invasive species (Schierenbeck, 2004; Whitehead and Bowers, 2013). These invasive honeysuckles have devastated the native ecosystem in many areas of eastern North America, and allelopathic metabolites have been suggested to contribute to their devastating effect (Cipollini et al., 2008a; Cipollini and Dorning 2008). The extract of *L. maackii* was also reported to affect the ecological dynamics of native fauna and mycorrhiza (Cipollini et al., 2008b; Watling et al., 2011). However, it is still unclear which compounds cause these ecological effects. Thus, an investigation on the phytochemical diversity in *Lonicera* species is warranted in the

* Corresponding author.
** Corresponding author.
E-mail addresses: kbkang@sookmyung.ac.kr (K.B. Kang), tjyang@snu.ac.kr (T.-J. Yang).
[1] Present address: Research Institute of Pharmaceutical Sciences, College of Pharmacy, Sookmyung Women's University, Seoul, 04310, Republic of Korea.
[2] Dedicated to the memory of our esteemed colleague Prof. Sang Hyun Sung, a good friend, inspiring mentor, and talented scientist who passed away much too early on July 24th, 2018.

https://doi.org/10.1016/j.phytochem.2018.07.012
Received 24 March 2018; Received in revised form 15 July 2018; Accepted 20 July 2018

fields of both pharmacology and ecology.

Recent advances in hyphenated chromatography techniques allow for simultaneous analyses of numerous metabolites in a short runtime. The UHPLC–Q/TOF–MS method, which comprises ultrahigh-performance liquid chromatography (UHPLC) and high resolution quadrupole time-of-flight mass spectrometry (Q/TOF–MS), has become the most common method for profiling specialized metabolites (also called secondary metabolites) in plant samples because it provides MS/MS fragmentation pattern data, which imply partially structural information of metabolites (Wolfender et al., 2015). Some previous studies applied the LC–MS approach for the metabolite profiles of *Lonicera* species: the leaves of *L. henryi* (Jaiswal et al., 2014), the caulis and flowers of *L. japonica* (Qi et al., 2009; Zhang et al., 2015), the berries of *L. caerulea* var. *kamtschatica* (Kucharska and Fecka, 2016; Kucharska et al., 2017), and the flowers of *L. japonica*, *L. macranthoides*, *L. confusa*, *L. hypoglauca*, *L. fulvotomentosa*, *L. similis*, *L. dasystyla*, and *L. syringantha* (Ren et al., 2008). These studies demonstrated that LC–MS is an efficient tool for profiling and identifying specialized metabolites in *Lonicera* plants, especially phenolic acids, flavonoids, and iridoids. However, most of them only applied the analytical dataset for quality control of the plant samples; a systemic approach to investigating diversity in specialized metabolism among *Lonicera* plants has not yet been utilized.

In the present study, the phylogenetic and phylochemical relationships between six *Lonicera* species occurring in Korea, *L. japonica*, *L. maackii*, *L. insularis*, *L. sachalinensis*, *L. praeflorens*, and *L. vesicaria* (abbreviated as Lj, Lm, Li, Ls, Lp, and Lv, respectively), were revealed to expand our systemic knowledge on this genus, in both of genomic and chemical characters. The genomic diversity among these species was investigated based on their chloroplast DNA and their taxonomic relationship was established. Additionally, the phytochemical compositions were profiled by LC–MS analyses on the aerial parts and roots of the tested species. We conducted the genomics study and metabolomics study together for the same individual plants of each species. Every plant sample was cultivated in the same place (Medicinal Plant Garden, College of Pharmacy, Seoul National University) and collected at the same time to minimize the environmental effect on specialized metabolic diversity. Performing this study, we expected to acquire relevant information regarding the management and utilization of this pharmacologically and ecologically plant genus.

2. Results and discussion

2.1. Genomic diversity and phylogeny among Lonicera species

The complete chloroplast genome sequences of six *Lonicera* species were obtained by assembly of approximately 1 Gbp of whole genome sequences for each species. The completely assembled sequences were ranged from 154,892 to 155,318 bp (GenBank nos. MH028738, Lj; MH028739, Li; MH028740, Lp; MH028741, Lm; MH028742, Ls; MH028743, Lv) (Table 1). Diverse polymorphism among these plants was revealed by the comparative analysis. We identified 17–2261 SNPs and 5–278 InDels between species. The lowest numbers of SNPs and InDels (17 and 5) were identified between *L. insularis* and *L. sachalinensis*a; meanwhile, the highest numbers of SNPs (2,261) were identified between *L. vesicaria* and *L. japonica* and the highest numbers of InDels (278) were identified between *L. insularis* and *L. japonica* (Table 2). The phylogenetic tree revealed that *L. japonica* is most diverse and grouped into an independent group (Fig. 1). *L. insularis* and *L. sachalinensis* were the closest, and they belonged to the same subgroup as *L. maackii*. *L. praeflorens* and *L. vesicaria* were classified into another subgroup.

2.2. Development of DNA marker to authenticate the Lonicera species

We developed a DNA marker, named as Lo_i_04, to validate the chloroplast genome sequence assembly and to serve a further application in the authentication of each species. PCR primers were developed for identifying the *Lonicera* species based on the copy number variation (CNV) of the tandem repeat units in the chloroplast genomes. The CNV-based InDel variation was estimated, and the PCR result coincided with the sequence-based estimation (Fig. 2). Using this DNA marker, the genomic diversity of *L. insularis*, *L. sachalinensis*, and *L. maackii* to other related species could be authenticated. These three species cannot be distinguished by this DNA marker alone; however, as mentioned above, many more SNPs and InDels between *Lonicera* species were characterized (Table 2). Thus, we expect that we could develop more DNA markers for establishing a practical authentication system for *Lonicera* species. Because of the increasing demands for *L. japonica* in the medicinal herb market, quality control has been an important issue for this species. Thus, an authentic DNA marker for identifying these species can be utilized to prevent adulteration or misuses of other *Lonicera* species as *L. japonica*.

2.3. Tentative identification of metabolites

The UHPLC–Q/TOF–MS analysis of the aerial parts and root extracts of six *Lonicera* species exhibited base peak ion (BPI) chromatograms as shown in Fig. 3. The MS^E method (Plumb et al., 2006) allowed us to acquire high-energy collision-induced dissociation (CID) MS data for tentative identification of the major chromatographic peaks. Flavonoids, phenolic acids, iridoids, and their glycosides have been closely investigated for their MS/MS fragmentation (Es-Safi et al., 2007; Fabre et al., 2001; Jaiswal et al., 2014; March et al., 2006); hence, many peaks could be tentatively identified based on their high-energy CID MS spectra as shown in Table 3. In our previous study, 13 iridoids and secoiridoids were isolated and identified from the roots of the Korean endemic species *L. insularis* (Kang et al., 2018); thus, these isolated compounds were also injected to confirm the identification of peaks **1**, **5**, **8**, **9**, **14**, **15**, **20**, **33**, **37**, and **48**. Details on the tentative identification are described in the Supplementary Data (Figs. S1–S23).

2.4. Chemotaxonomy among Lonicera species samples

1471 MS ion markers were extracted from the LC–MS dataset, and a principal component analysis (PCA) was performed with them to analyze the chemodiversity among samples. A PCA model with three principle components (PC) was established in which PC1, PC2, and PC3 accounted for 20.3%, 17.4%, and 13.4% of the total variance, respectively (Supplementary Data, Fig. S24a). The PC1-PC2 score plot (Fig. 4a) showed that every sample was distributed in the Hotelling's T^2 95% confidence ellipse, which means the analysis did not contain any outlier. The aerial parts and roots of *L. praeflorens* were separately grouped from the other species, with positive PC1 and negative PC2 values. The PC1-PC2 loading plot (Fig. 4b) revealed that this separation was caused by the relatively high content of loganic acid (**1**) in *L. praeflorens*. This could also be ascertained in the BPI chromatograms (Fig. 3) and the MarkerLynx ion marker table in which the ion intensities of loganic acid in the *L. praeflorens* samples were more than five times higher than those of the other species. Iridoid glycosides are well-known as plant derived defense metabolites against herbivores or pathogen (Dobler et al., 2011). Whitehead and Bowers revealed that in *Lonicera* plants, iridoid glycosides show significantly higher concentrations in fruits than in leaves, which was suggested to defend fruits against antagonistic seed predators and fruit pathogens (Whitehead and Bowers, 2013). *L. praeflorens* bear fruits between May and June while most of other *Lonicera* species bear fruits between July and August ("*praeflorens*" means flowering early). Plant samples used in this study were harvested in early July, so it could be suggested that *L. praeflorens* biosynthesized significantly higher amount of iridoid glycosides, especially loganic acid, to defend fruits. In the PC1-PC3 score plot (Fig. 4c), the roots and aerial parts of *L. vesicaria* were separated from the other

Table 1
Statistics of WGS and assembly summary for six *Lonicera* species.

Feature	*L. insularis*	*L. sachalinensis*	*L. praeflorens*	*L. maackii*	*L. vesicaria*	*L. japonica*
Sequencing information						
No. of raw read	4,941,334	4,764,738	4,342,742	4,920,926	5,596,064	6,308,194
No. of trimmed read	4,662,540	4,339,126	4,024,338	4,640,648	4,712,150	5,029,201
No. of trimmed bases	1,211,552,506	1,098,408,065	1,040,146,882	1,188,483,775	1,164,886,321	1,178,414,508
Chloroplast genome						
Average read depth	634.83	214.83	165.39	784.00	134.00	668.84
Genome size (bp)	155,124	155,123	154,892	155,318	155,182	155,060
Large single copy	88,230	88,229	88,353	89,202	89,096	88,853
Small single copy	18,774	18,774	18,929	18,680	18,612	18,653
Inverted repeat	24,060	24,060	23,805	23,718	23,737	23,777
Number of genes	114	114	114	114	113	109
Protein-coding genes	80	80	80	80	79	77
Structure RNAs	34	34	34	34	34	32
GC contents (%)	38.35	38.34	38.31	38.47	38.39	38.59
GenBank acc. no.	MH028739	MH028742	MH028740	MH028741	MH028743	MH028738

Table 2
Summary of SNPs and InDels found in chloroplast genomes among the six *Lonicera* species.

Species		Indel					
		Li	Ls	Lp	Lm	Lv	Lj
SNP	**Li**	/	5	246	153	247	278
	Ls	17	/	246	156	245	277
	Lp	1450	1439	/	227	235	271
	Lm	754	743	1426	/	223	266
	Lv	1550	1539	1446	1490	/	268
	Lj	1964	1953	2072	1958	2261	/

The upper triangle shows the number of indel, while the lower triangle indicates the total nucleotide substitutions Abbreviations: Li, *L. insularis*; Ls, *L. sachalinensis*; Lp, *L. praeflorens*; Lm, *L. maackii*; Lv, *L. vesicaria*; Lj, *L. japonica.*

species by their PC3 values. *L. vesicaria* showed relatively high contents of dicaffeoylquinic acids (**27** and **31**) and grandifloroside (**34**), which was suggested by the PC1-PC3 loading plot (Fig. 4d). The BPI chromatogram of the *L. vesicaria* roots supported this, showing especially high intensity of peak **34**. For the other samples, the roots and aerial parts tended to be separated in the scatter plots (Fig. 4a and c).

For further investigation of the chemical diversity among the *Lonicera* species, additional PCAs were performed within the aerial parts and roots separately. In the PCA model within six *Lonicera* roots (Fig. 5a and b), in which PC1, PC2, and PC3 accounted for 30.4%, 24.7%, and 19.1% of the total variance respectively (Supplementary Data, Fig. S24b), the samples showed a different distribution of iridoid and secoiridoid derivatives. *L. praeflorens* and *L. vesicaria* showed similar patterns to the first PCA result, showing significantly high contents of loganic acid (**1**) (Lp), and dicaffeoylquinic acids (**27** and **31**) and grandifloroside (**34**) (Lv). 7-Desmethylsecologanol (**3**) was also abundant in *L. praeflorens*. *L. insularis* and *L. sachalinensis* exhibited very similar metabolite profiles, in which periclymenoside (**37**), kinginoside (**48**), and methylgrandifloroside methyl ester (**49**) showed high ion intensities. These three compounds and grandifloroside (**34**) share a structural trait; they commonly contain a feruloyl moiety in their structures. Periclymenoside and kinginoside have been reported from only a small number of *Lonicera* species, *L. periclymenum* (Calis et al., 1984), *L. morrowii* (Aimi et al., 1993), and *L. insularis* (Kang et al., 2018). From these, it could be proposed that the biosynthetic ability for feruloyl iridoid derivatives recently appeared during the speciation of these species. *L. maackii* showed a relative abundance of sweroside (**9**). PC3 did not show a significant difference between species (Supplementary Data, Figs. S25a and S25b).

Another PCA model was established within the LC–MS dataset from the aerial parts of five *Lonicera* species (Fig. 5c and d). In this mode, PC1, PC2, and PC3 accounted for 34.2%, 21.6%, and 18.7% of the total variance (Supplementary Data, Fig. S24c). However, PC1 majorly shows the variance between *L. praeflorens* and other species which were already investigated in Fig. 4 (Supplementary Data, Figs. S25c and S25d); thus, further variance between other five species were visualized using PC2-PC3 plots. The aerial parts of *L. sachalinensis* showed a significant abundance of periclymenoside (**37**) and methylgrandifloroside methyl ester (**49**) as similar to the root sample, whereas the aerial parts of *L. insularis* exhibited a different chemical profile. *L. insularis* and *L. mackii* showed similar chemical profiles which were relatively abundant in secologanic acid (**5**) and unidentified iridoid derivatives (**13** and **18**). *L. japonica* showed relatively high contents of flavonoids and phenolic acids, such as luteolin 7-*O*-(6-*O*-rhamnosylhexoside) (**24**), 3,4-di-*O*-caffeoylquinic acid (**27**), and apigenin 7-*O*-(6-*O*-glucosylrhamnoside) (**30**). Sweroside (**9**) was identified as a chemical marker for

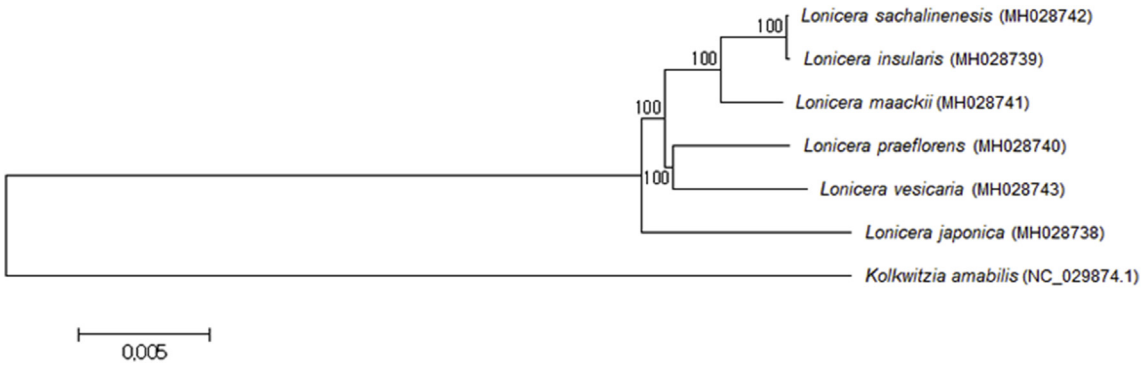

Fig. 1. Phylogenetic analysis of six *Lonicera* species based on complete chloroplast genome. The tree was generated by multiple alignment using MAFFT and a neighbor-joining (Chen et al., 2017) analysis using MEGA 6.0. The numbers in the nodes indicate bootstrap support values.

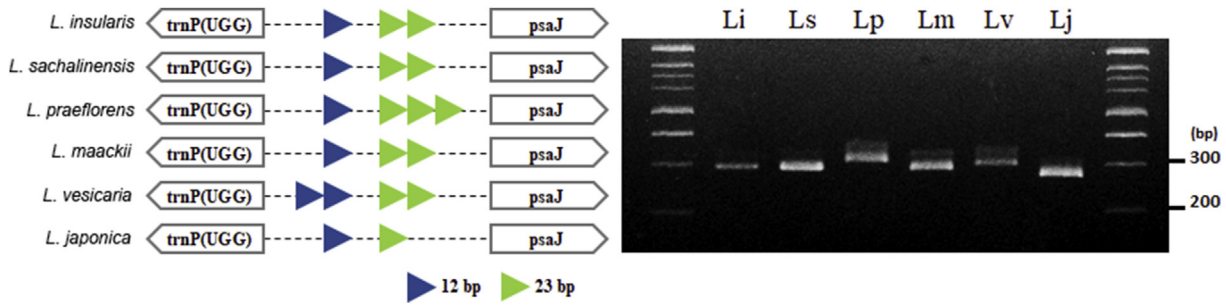

Fig. 2. An InDel marker (Lo_i_04) for authentication of six *Lonicera* species based on copy number variation (CNV) in the intragenic region. The InDel marker was developed based on chloroplast genome sequences of six *Lonicera* species and successfully validated by PCR. The PCR primer pairs were 5′-AAACAAACGCGCTAC CAAGC-3′ and 5′-CCCGAGCATTCCCGAAAAAG-3′. Li, *L. insularis*; Ls, *L. sachalinensis*; Lp, *L. praeflorens*; Lm, *L. maackii*; Lv, *L. vesicaria*; Lj, *L. japonica*.

L. maackii in the root sample based the PCA model, but in the aerial parts it was accumulated abundantly in *L. sachalinensis* and *L. vesicaria*.

The chemotaxonomic relationship among *Lonicera* species was established by a hierarchical clustering analysis (HCA) among 12 samples (Fig. 6). The distances between samples were calculated using Ward's method and Euclidian metrics, and the tree was sorted by size. The samples were divided into three groups: the roots and aerial parts of *L. praeflorens*, the aerial parts of the other species, and the roots of the other species. As shown in the PC1-PC2 score plot, the chemical contents of *L. praeflorens* were quite different from that of the other five species. The chemophylogeny among the roots did not correspond to one between the aerial parts or to the phylogenetic tree based on the chloroplast DNA sequences. This type of discordance between genotypes and chemotypes is common because plant specialized metabolite phenotypes are determined by the complex contribution and interaction of genotype and environmental effects (Chen et al., 2015; Hamilton et al., 2001). Nevertheless, some partial consistency can still be found in the phylogenetic and phylochemical trees; for example, the roots of *L. insularis* and *L. sachalinensis* exhibited similar chemical profiles. *L. insularis*, *L. sachalinensis*, and *L. maackii* formed a cluster for their aerial part metabolites, as they did in the chloroplast genome-based phylogenetic tree.

2.5. Metabolite localization in Lonicera species

To further investigate the chemical diversity among the *Lonicera* samples, additional multivariate analysis models were established. At first, based on the PCA and HCA results, an orthogonal projections to latent structures discriminant analysis (OPLS-DA) model was built with ten samples except *L. praeflorens* to examine the metabolic difference between the aerial parts and roots of *Lonicera* plants. The OPLS-DA model exhibited an acceptable predictability, showing R^2 and Q^2 values of 0.989 and 0.755, respectively. The OPLS-DA score plot and the *S*-plot were used for visualization of the ion markers that influenced the model (Fig. 7). Several iridoid derivatives showed a significantly higher content in the roots, such as 7-desmethylsecologanol (**3**), sweroside (**9**), (*E*)-aldosecologanin (**33**), and grandifloroside (**34**), whereas the flavonoids (**23** and **29**) tended to subsist in the aerial parts. Interestingly, secologanin (**5**) is a secoiridoid derivative, but it showed a high content in the aerial parts of *Lonicera* species rather than in their roots. We could set two hypothesis for this characteristic localization of secologanin. As mentioned above, iridoid glycosides are well-known as plant derived defense metabolites. Peñuelas and coworkers reported that eggs of the herbivore *Euphydryas aurinia* significantly increased the concentration of iridoid glycosides in leaves of *Lonicera implexa*, and

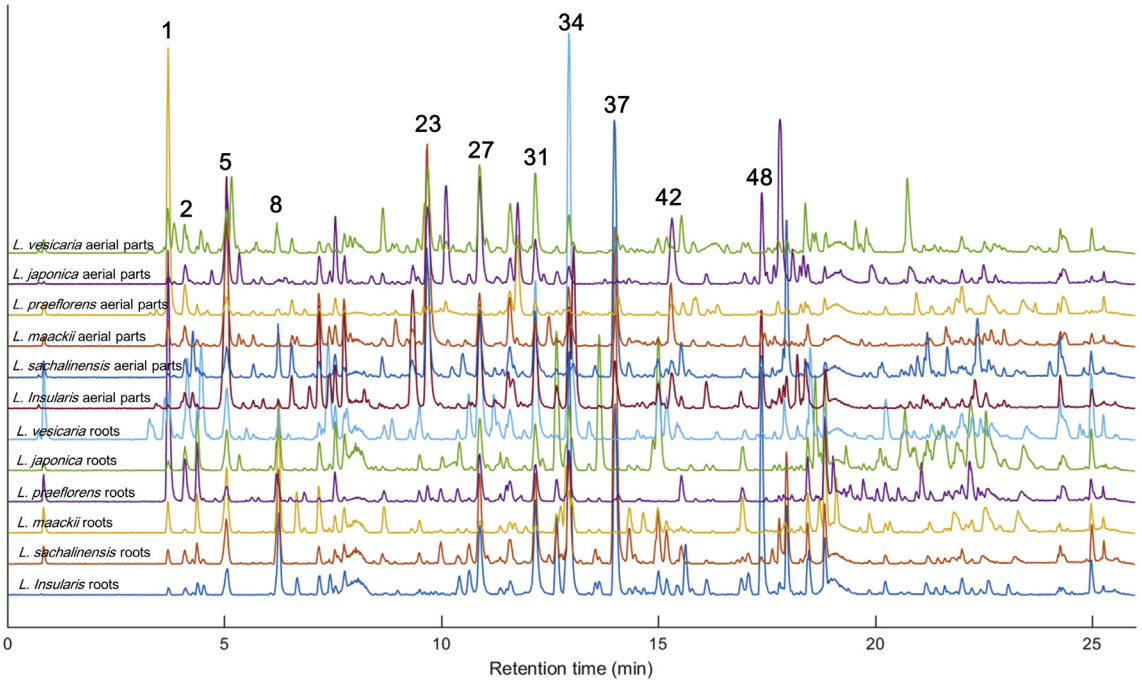

Fig. 3. LC–MS base peak ion (BPI) chromatograms of the root and aerial part extracts of six *Lonicera* species. Some major chromatographic peaks are marked with their peak numbers.

Table 3
Characterization of metabolites in *Lonicera* plant extracts by LC–MS.

No.	Identity	Classification	t_R (min)	Observed MS $[M-H]^-$	Calculated MS $[M-H]^-$	Molecular formula	Fragments
1	loganic acid[a]	Iridoid	3.71	375.1286	375.1291	$C_{16}H_{24}O_{10}$	213 $[M-Glc-H_2O-H]^-$ 169 $[M-Glc-COOH-H]^-$ 151 $[M-Glc-COOH-H_2O-H]^-$
2	quinic acid	organic acid	4.07	191.0554	191.0556	$C_7H_{12}O_6$	–
3	7-desmethylsecologanol	Iridoid	4.38	375.1270	375.1291	$C_{16}H_{24}O_{10}$	309, 265, 195, 151
4	unknown	unknown	4.53	469.1454	469.1499	$C_{25}H_{26}O_9$	237, 193
5	secologanic acid[a]	Iridoid	5.07	373.1127	373.1135	$C_{16}H_{22}O_{10}$	193 $[M-Glc-H_2O-H]^-$
6	unknown	unknown	5.17	369.0806	369.0822	$C_{16}H_{18}O_{10}$	207, 192
7	unknown	unknown	5.33	507.1717	507.1714	$C_{21}H_{32}O_{14}$	–
8	loganin[a]	Iridoid	6.19	389.0858	389.0873	$C_{19}H_{18}O_9$	227 $[M-Glc-H]^-$
9	sweroside[a]	Iridoid	6.26	357.1182	357.1186	$C_{16}H_{22}O_9$	195 $[M-Glc-H]^-$ 125 $[(RDA\ product)-H]^-$
10	unknown	unknown	6.54	519.2454	519.2442	$C_{24}H_{40}O_{12}$	441, 207
11	6′-*O*-apiosylsweroside	Iridoid	6.68	489.1610	489.1608	$C_{21}H_{30}O_{13}$	195 $[M-Api-Glc-H]^-$ 125 $[(RDA\ product)-H]^-$
12	luteolin 7-*O*-(6-*O*-glucosylglucoside)	flavonoid	6.97	609.1474	609.1456	$C_{27}H_{30}O_{16}$	447 $[M-Glc-H]^-$ 285 $[M-2Glc-H]^-$
13	unknown	Iridoid	7.18	419.1531	419.1553	$C_{18}H_{28}O_{11}$	–
14	secologanol[a]	Iridoid	7.36	389.1467	389.1448	$C_{17}H_{26}O_{10}$	–
15	secologanin[a]	Iridoid	7.41	387.1288	387.1291	$C_{17}H_{24}O_{10}$	225 $[M-Glc-H]^-$ 155 $[(RDA\ product)-H]^-$
16	unknown	phenyl propanoid	7.45	503.1772	503.1765	$C_{22}H_{32}O_{13}$	287, 155
17	Kingiside	iridoid	7.55	403.1245	403.1240	$C_{17}H_{24}O_{11}$	–
18	unknown	Iridoid	7.77	387.1277	387.1267	$C_{17}H_{24}O_{10}$	255, 155
19	unknown	unknown	8.67	579.2056	579.2078	$C_{28}H_{36}O_{13}$	417, 181
20	7-desoxyloganic acid[a]	iridoid	8.69	359.1333	359.1342	$C_{16}H_{24}O_9$	197 $[M-Glc-H]^-$
21	luteolin 7-*O*-(6-*O*-arabinosylglucoside)	flavonoid	8.96	579.1351	579.1350	$C_{26}H_{28}O_{15}$	447 $[M-Ara-H]^-$ 285 $[M-Ara-Glc-H]^-$
22	miscanthoside	flavonoid	9.33	449.1084	449.1084	$C_{21}H_{22}O_{11}$	287 $[M-Glc-H]^-$ 151 ($^{1,3}A^-$ of aglycone) 135 ($^{1,3}B^-$ of aglycone)
23	luteolin-7-*O*-glucoside	flavonoid	9.69	447.0916	447.0927	$C_{21}H_{20}O_{11}$	285 $[M-Glc-H]^-$
24	lonicerin	flavonoid	10.11	593.1511	593.1506	$C_{27}H_{30}O_{15}$	447 $[M-Rha-H]^-$ 285 $[M-Rha-Glc-H]^-$
25	unknown	unknown	10.43	743.2420	743.2399	$C_{33}H_{44}O_{19}$	–
26	3,5-di-*O*-caffeoylquinic acid	organic acid	10.65	515.1194	515.1190	$C_{25}H_{24}O_{12}$	375 $[M-(caffeoyl)+HCOOH-H]^-$ 353 $[M-(caffeoyl)-H]^-$ 335 $[M-(caffeoyl)-H_2O-H]^-$ 191 $[M-2(caffeoyl)-H]^-$ 179 $[(caffeic\ acid)-H]^-$ 135 $[(caffeic\ acid)-CO_2]^-$
27	3,4-di-*O*-caffeoylquinic acid	organic acid	10.88	515.1188	515.1190	$C_{25}H_{24}O_{12}$	(similar to **26**)
28	luteolin-4′-*O*-glucoside	flavonoid	11.54	447.0921	447.0927	$C_{21}H_{20}O_{11}$	285 $[M-Glc-H]^-$
29	apigenin 7-*O*-glucoside	flavonoid	11.59	431.0981	431.0978	$C_{21}H_{20}O_{10}$	268 $[M-Glc-H]^-$
30	apigenin 7-*O*-(2-*O*-glucosylrhamnoside)	flavonoid	11.75	577.1551	577.1557	$C_{27}H_{30}O_{14}$	413 $[M-Glc-H]^-$, 269 $[M-Glc-Rha-H]^-$
31	4,5-di-*O*-caffeoylquinic acid	organic acid	12.17	515.1197	515.1190	$C_{25}H_{24}O_{12}$	(similar to **26**)
32	unknown	unknown	12.48	505.2647	505.2649	$C_{24}H_{42}O_{11}$	373, 161
33	(*E*)-aldosecologanin[a]	iridoid	12.66	757.2552	757.2555	$C_{34}H_{46}O_{19}$	595 $[M-Glc-H]^-$ 525 $[(RDA\ Product)-H]^-$
34	grandifloroside	iridoid	12.94	537.1614	537.1614	$C_{25}H_{30}O_{13}$	375 $[M-(caffeoyl)-H]^-$ 179 $[(caffeic\ acid)-H]^-$
35	hesperetin	flavonoid	13.05	301.0711	301.0712	$C_{16}H_{14}O_6$	–
36	(*Z*)-alcosecologanin	iridoid	13.66	757.2563	757.2555	$C_{34}H_{46}O_{19}$	(similar to **33**)
37	periclymenoside[a]	iridoid	14.00	727.2451	727.2449	$C_{33}H_{44}O_{18}$	565 $[M-Glc-H]^-$ 403 $[M-2Glc-H]^-$ 193 $[(ferulic\ acid)-H]^-$
38	unknown	unknown	14.32	733.2334	733.2344	$C_{35}H_{42}O_{17}$	537, 357, 177
39	3-*O*-caffeoylquinic acid	organic acid	14.51	353.0871	353.0873	$C_{16}H_{18}O_9$	191 $[M-(caffeoyl)-H]^-$ 179 $[(caffeic\ acid)-H]^-$
40	7-*O*-(*Z*)-feruloylloganic acid	iridoid	14.88	551.1734	551.1765	$C_{26}H_{32}O_{13}$	389 $[M-Glc-H]^-$ 193 $[(ferulic\ acid)-H]^-$
41	7-*O*-(*E*)-feruloylloganic acid	iridoid	15.01	551.1734	551.1765	$C_{26}H_{32}O_{13}$	(similar to **40**)
42	luteolin	flavonoid	15.32	285.0403	285.0399	$C_{15}H_{10}O_6$	–
43	unknown	unknown	15.53	705.2971	705.2970	$C_{32}H_{50}O_{17}$	347
44	unknown	unknown	15.63	799.4874	799.4844	$C_{42}H_{72}O_{14}$	–
45	lonitoside	terpenoid	16.11	461.1998	461.2023	$C_{21}H_{34}O_{11}$	347
46	unknown	unknown	16.93	703.2240	703.2238	$C_{34}H_{40}O_{16}$	345, 327, 315
47	unknown	unknown	17.09	539.1765	539.1765	$C_{25}H_{32}O_{13}$	359, 167
48	kinginoside[a]	iridoid	17.39	679.2232	679.2238	$C_{32}H_{40}O_{16}$	537, 483, 441, 381, 339 193 $[(ferulic\ acid)-H]^-$

(*continued on next page*)

Table 3 (*continued*)

No.	Identity	Classification	t_R (min)	Observed MS $[M-H]^-$	Calculated MS $[M-H]^-$	Molecular formula	Fragments
49	methylgrandifloroside methyl ester	iridoid	17.95	565.1916	565.1921	$C_{27}H_{34}O_{13}$	403 $[M-Glc-H]^-$ 371 $[M-(feruloyl)-H]^-$ 193 $[(ferulic\ acid)-H]^-$
50	onjixanthone I	xanthone	18.22	301.0710	301.0712	$C_{16}H_{14}O_6$	–
51	unknown	biflavonoid	18.39	537.0839	537.0822	$C_{30}H_{18}O_{10}$	417, 375
52	unknown	fatty acid	18.83	329.2325	329.2328	$C_{18}H_{34}O_5$	–
53	unknown	biflavonoid	18.86	537.0836	537.0822	$C_{30}H_{18}O_{10}$	417, 375

[a] Confirmed by comparison with previously isolated compounds.

secologanic acid was the most abundant derivative (Peñuelas et al., 2006). Based on these facts, we could hypothesize that secologanin was localized at leaves, because it might have specific selectivity against herbivores than other iridoid glycosides. Another hypothesis was related to the biosynthetic pathway of secoiridoids; secologanin is known to be formed by the oxidative cleavage of loganin, which is catalyzed by secologanin synthase (SLS) (Irmler et al., 2000). Despite early studies on the secoiridoid biosynthesis pathway, especially the identification of SLS performed with suspension cultured cells of *L. japonica* (Yamamoto et al., 1999, 2000), little is known about the gene expression, protein localization, and metabolite accumulation involved with secoiridoid biosynthesis in *Lonicera* plants. Y. Liu and coworkers showed that the expression of the *SLS2* gene is higher in the stems, leaves, and flowers than in the roots in the case of the Tibetan medicinal plant *Swertia mussotii* (Liu et al., 2017). This was contrary to the high expression of *SLS1* and *SLS2* in *Catharanthus roseus* roots (de Bernonville et al., 2015), which suggests that the localization of SLS can differ across plant taxa. A. Rai and coworkers reported a significantly high expression of *SLS* in the young leaf tissues of *L. japonica*, but they did not use the root tissue in the study (Rai et al., 2017). Thus, it could be hypothesized that in the case of *Lonicera* plants, *SLS* is localized in the leaves while other iridoid biosynthetic cascades are localized in the roots. However, further investigation is required to confirm these hypotheses on localization of secologanin in *Lonicera*.

3. Conclusion

The present study revealed a significant difference in diversity among the six *Lonicera* species tested in Korea according to the chemical and genomic analyses. Because the genome sequences used in this study were neutral, they cannot be correlated with the biosynthetic diversity among these species; however, we could develop an Indel-based DNA barcode which can be used for authentication of these plants. Recently, Gao and coworkers revealed that *L. japonica* flowers in China were seriously adulterated and counterfeited, using the DNA barcoding method (Gao et al., 2017); thus, the result of this study will be helpful to broaden the application of DNA barcoding in quality assessments of this important medicinal herb. The chemical analyses showed that the specialized metabolites of these species are not very different qualitatively but rather very different quantitatively. The

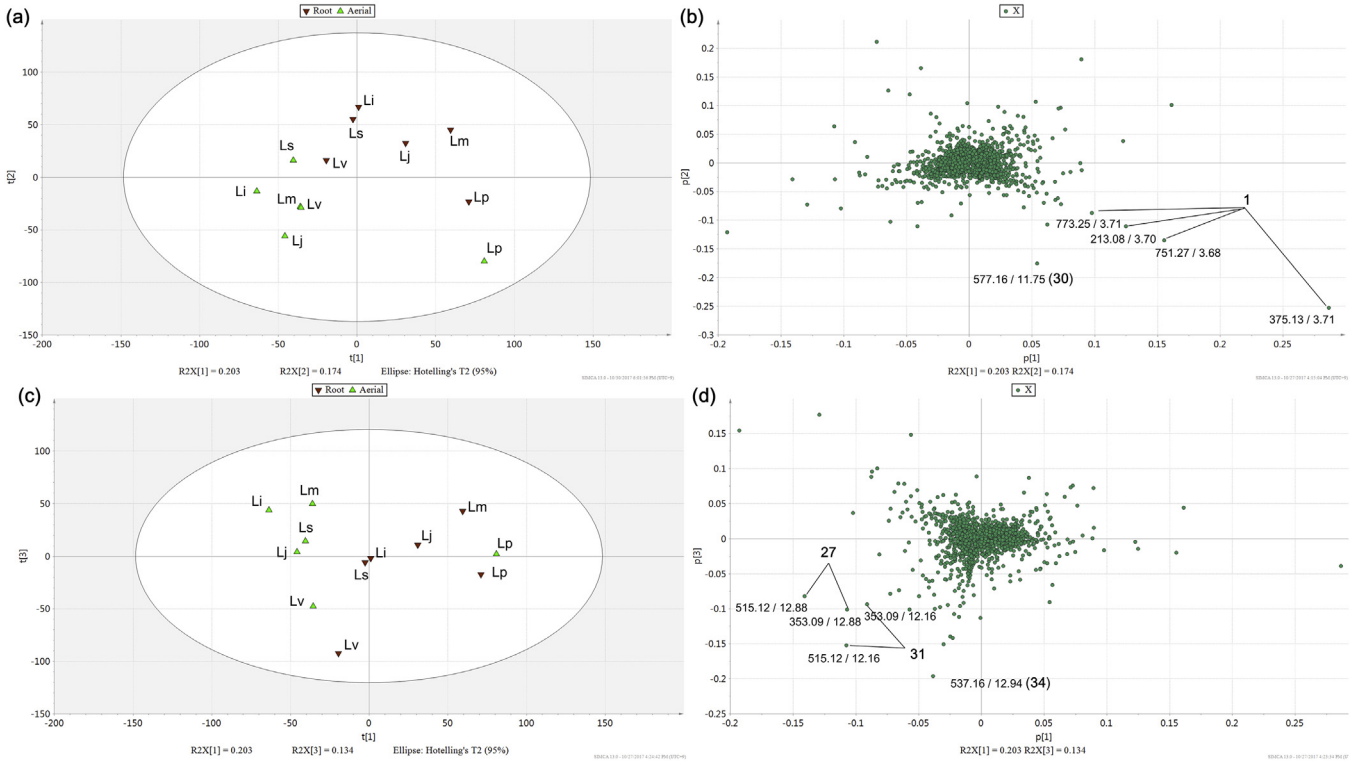

Fig. 4. PC1-PC2 (a) score plot and (b) loading plot, and the PC1-PC3 (c) score plot and (d) loading plot of the PCA model established with the LC–MS ion marker dataset. In the score plots, green triangles and brown inverted triangles correspond to aerial parts and roots, respectively. In the loading plots, some important markers are labelled with xxx/yy, in which xxx means *m/z* values and yy means retention time. Li, *L. insularis*; Ls, *L. sachalinensis*; Lp, *L. praeflorens*; m, *L. maackii*; Lv, *L. vesicaria*; Lj, *L. japonica*. (For interpretation of the references to colour in this figure legend, the reader is referred to the Web version of this article.)

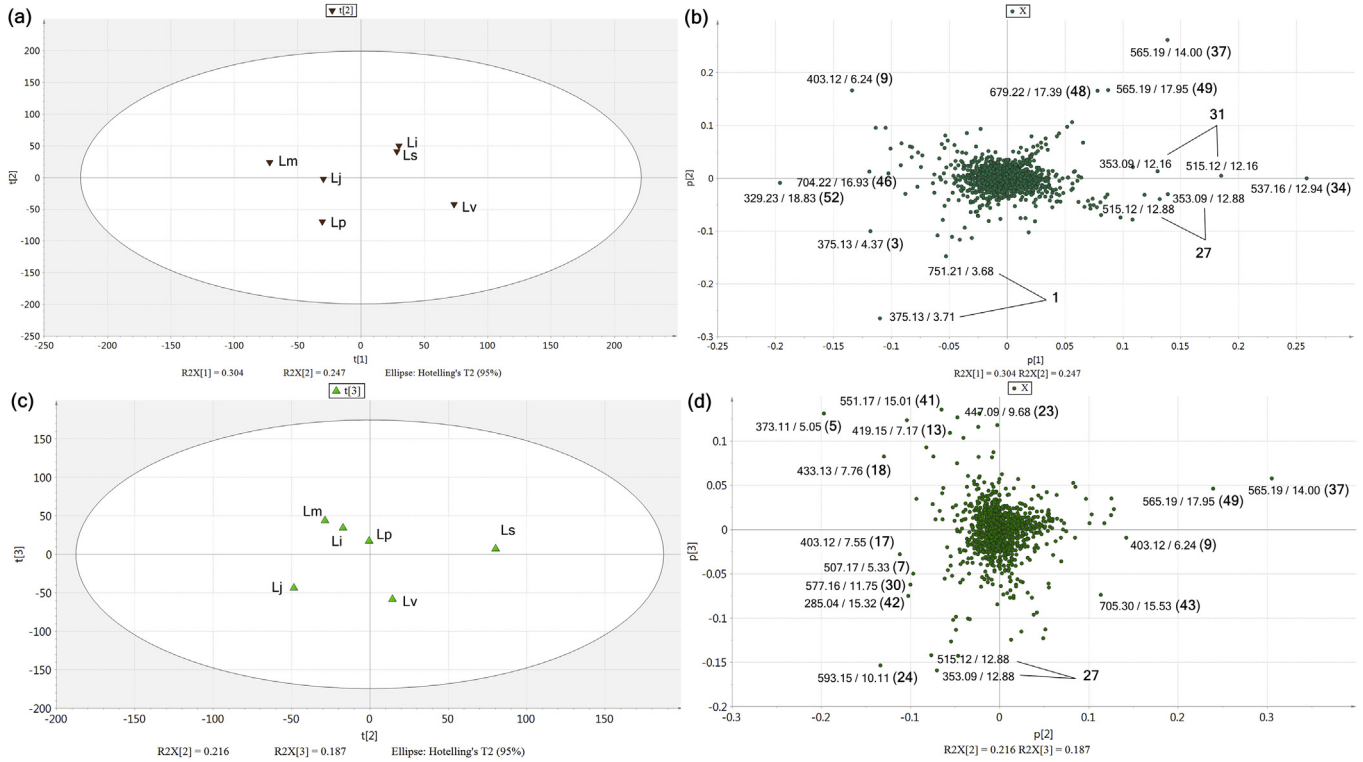

Fig. 5. PC1-PC2 (a) Score plot and (b) loading plot of the PCA model established with LC–MS ion marker dataset of 6 *Lonicera* root extracts, and PC2-PC3 (c) score plot and (d) loading plot of the PCA model of 6 aerial part extracts. In the loading plots, some important markers are labelled with xxx/yy, in which xxx means *m/z* values and yy means retention time. Li, *L. insularis*; Ls, *L. sachalinensis*; Lp, *L. praeflorens*; Lm, *L. maackii*; Lv, *L. vesicaria*; Lj, *L. japonica*.

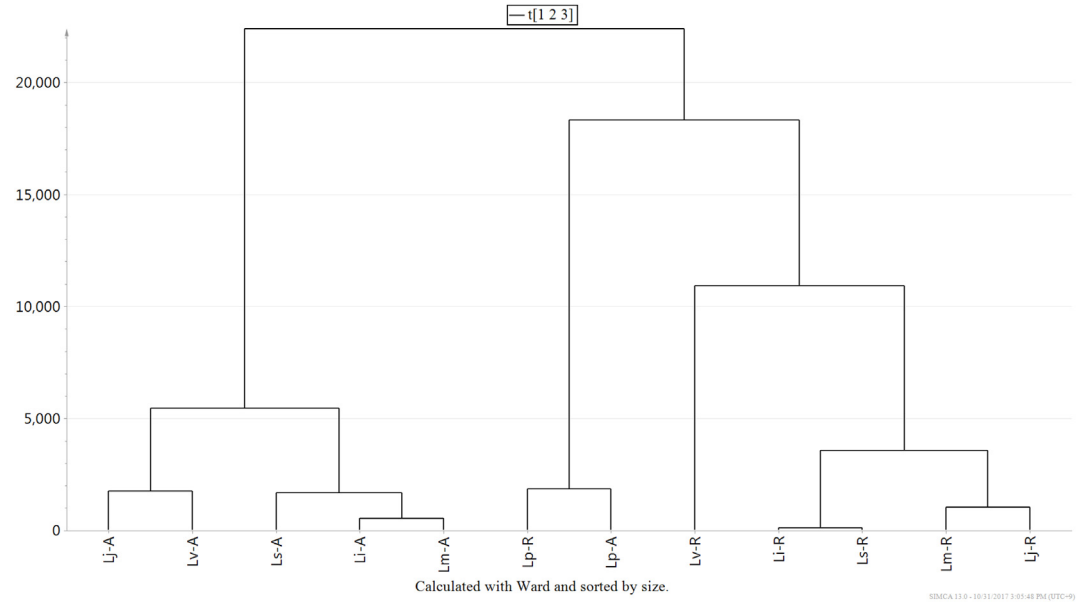

Fig. 6. Dendrogram obtained from HCA with the LC–MS dataset of 12 *Lonicera* extracts. The distances between samples were calculated using Ward's method and Euclidian metrics, and the tree was sorted by size. Li, *L. insularis*; Ls, *L. sachalinensis*; Lp, *L. praeflorens*; Lm, *L. maackii*; Lv, *L. vesicaria*; Lj, *L. japonica*. A, aerial parts; R, roots.

analytical data provided us with implications about metabolic diversity in the *Lonicera* species tested, especially for iridoid and secoiridoid glycosides. *L. praeflorens* exhibited a significantly different chemical profile to the other species, and we suggest that this is linked to the early fruiting character of *L. praeflorens*, based on the ecological role of iridoid glycosides as feeding deterrents. To the best of our knowledge, this is the first report about chemical diversity in *Lonicera* species, including five species other than *L. japonica* which have hardly been investigated for their genomic and chemical diversity. The genomic and chemical profiles revealed in this study will provide valuable information for future studies in *Lonicera* species which are important in both of ecological and pharmacological aspects. We expect that genetic and chemical markers established in this study could be used for prevention of misuse of other *Lonicera* species as *L. japonica* in herbal markets, and they also could contribute to ecological studies, especially for plant-herbivore chemical interactions and invasion biology.

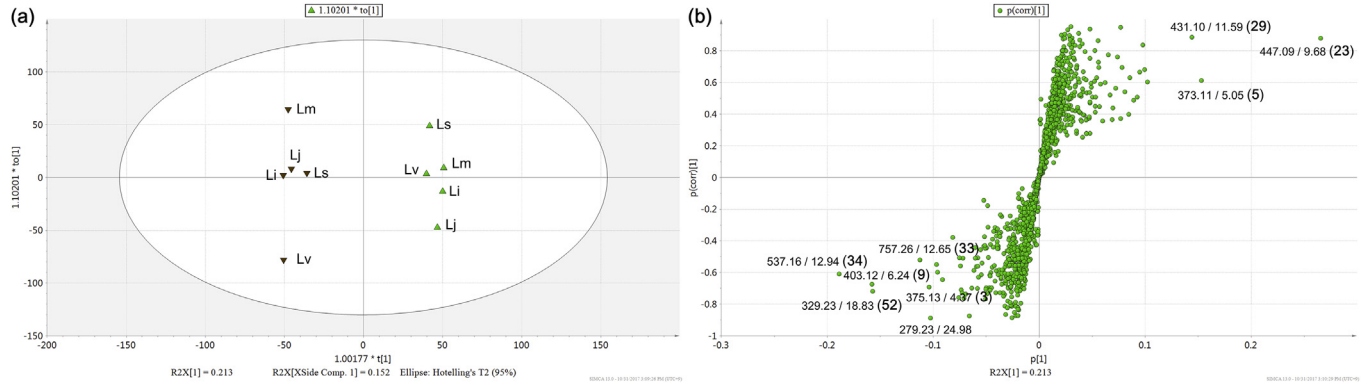

Fig. 7. (a) Score plot and (b) *S*-plot of the OPLS-DA model for aerial part and root extracts of five *Lonicera* species (*L. praeflorens* was excluded). Li, *L. insularis*; Ls, *L. sachalinensis*; Lm, *L. maackii*; Lv, *L. vesicaria*; Lj, *L. japonica*.

4. Experimental

4.1. Chemicals and reagents

HPLC grade water and acetonitrile (MeCN) were purchased from Avantor Performance Materials, Inc. (Center Valley, PA, USA). Formic acid and leucine-enkephalin were purchased from Sigma-Aldrich (St. Louis, MO, USA). Ultrapure water was triple deionized (Millipore, Bedford, MA, USA). MeOH was purchased from Daejung Chemicals Co., Ltd. (Siheung, Korea).

4.2. Plant materials

The Lonicera (Caprifoliaceae)species *L. japonica*, *L. maackii*, *L. insularis*, *L. sachalinensis*, *L. praeflorens*, and *L. vesicaria* were cultivated at the Medicinal Plant Garden, College of Pharmacy, Seoul National University, Koyang, Korea (GPS N37°42′42.9″, E126°49′10.6″), and collected in July 2015. The sample was authenticated by Mr. S. I. Han (Medicinal Plant Garden, College of Pharmacy, Seoul National University), and voucher specimens (SUPH-1507-L-01–12) were deposited in the Herbarium of the Medicinal Plant Garden.

4.3. Sample preparation

4.3.1. DNA extraction and whole genome shotgun (WGS) sequencing

High-quality genomic DNA of the six *Lonicera* species was obtained from fresh leaves using a modified cetyltrimethylammonium bromide (CTAB) method (Allen et al., 2006). The DNA concentration was examined by agarose gel electrophoresis and UV-spectrophotometer (Thermo Scientific Nanodrop ND-1000). The paired-end (PE) library was constructed using Ilumina MiSeq platform (Illumina, San Diego, CA).

4.3.2. Sample preparation for UHPLC–Q/TOF–MS analysis

The samples were divided into aerial parts and roots after drying. For each dried sample of 2.0–3.0 g, 80% MeOH (10 × sample weight) was added and extracted in a supersonic bath at room temperature (90 min, three times). These samples were centrifuged at 14,000 rpm for 3 min, and 1.0 mL of the supernatants was collected and loaded into Sep-Pak plus C_{18} solid-phase extraction cartridges (Waters CO., Milford, MA, USA) which were preconditioned with 5 mL of MeOH and 5 mL of water. The cartridges were washed with 6.0 mL of water and then eluted with 6.0 mL of MeOH. The eluates were filtered through Minisart RC 15 0.20 μm filters (Sartorius Stedim Biotech, Göttingen, Germany) prior to the LC–MS analyses.

4.4. Chloroplast genome sequence & phylogenetic analysis

The complete chloroplast genome sequences were assembled based on Illumina platform whole genome sequences (GenBank nos. MH028738, Lj; MH028739, Li; MH028740, Lp; MH028741, Lm; MH028742, Ls; MH028743, Lv). Complete chloroplast genome sequences were assembled by *de novo* assembly using Low-Coverage Whole genome sequence (dnaLCW) method using the CLC genome assembler (ver. beta 4.6, CLC Inc, Aarhus, Denmark) as reported previously (Kim et al., 2015, 2017). The gene annotation of the complete chloroplast genomes was performed using GeSeq (https://chlorobox.mpimp-golm.mpg.de/geseq.html) and manually confirmed using Artemis program and BLAST searches (Altschul et al., 1990). The chloroplast genome sequences of six *Lonicera* species were aligned by MAFFT program (https://mafft.cbrc.jp/alignment/server/), and then the phylogenetic analysis was constructed by the neighbor-joining (NJ) method with 1000 bootstrap values in MEGA 6.0 (Tamura et al., 2013).

4.5. Development and amplification of DNA marker

A primer for the co-dominant marker was developed from intergenic region between *trnP(UGG)* and *psaJ* genes, and designed using the primer-BLAST program (https://www.ncbi.nlm.nih.gov/tools/primer-blast/) (Altschul et al., 1990). PCR was conducted in a 25 μL reaction volume, and the amplification conditions were as follows: 94 °C for 5 min; 35 cycles of 94 °C, 58 °C and 72 °C for 30 s each, and then 72 °C for 7 min. The amplified fragments were analyzed in 3% agarose gel for 50 min. The gel was stained with ethidium bromide and visualized under UV.

4.6. UHPLC–Q/TOF–MS analysis

The LC–MS analyses were performed on a Waters Acquity UPLC system (Waters Co., Milford, MA, USA) coupled to a Waters Xevo G2 QTOF mass spectrometer (Waters MS Technologies, Manchester, UK) which was equipped with an electrospray ionization interface (ESI). Chromatographic separations were performed on a Waters Acquity UPLC BEH C_{18} (100 mm × 2.1 mm, 1.7 μm) column. The mobile phase comprised H_2O (A) and MeCN (B) with an optimized gradient as follows: 5–12% B (0–5 min); 12–25% B (5–16 min); 25–45% B (16–18 min); and 45–90% B (18–24 min), followed by 2 min of washing and reconditioning. The flow rate of the mobile phase was 0.3 mL/min, and the column temperature was maintained at 40 °C. Analyses of the samples (2.0 μL injected into the partial loop in the needle overfill mode) were performed in the negative ion modes in the *m/z* 50–1200 Da range with acquisition times of 0.2 s in the centroid mode. The ESI conditions were set as follows: capillary voltage 2.0 kV, con voltage 50 V, source temperature 120 °C, desolvation temperature

350 °C, cone gas flow 50 L/h, and desolvation gas flow 800 L/h. High-purity nitrogen was used as the nebulizer and auxiliary gas, and argon was used as the collision gas. The $[M - H]^-$ ion of leucine encephalin at *m/z* 554.2615 was used as the lock mass to ensure mass accuracy and reproducibility. The MS^E methodology was applied to acquire high-energy CID MS spectra for tentative identification of the metabolites (Plumb et al., 2006). The low collision energy for the detection of the precursor ions was set to 3 eV while the high collision energy for fragmentation was set to 40–45 eV.

4.7. LC–MS data preprocessing and multivariate analyses

MS ion markers were extracted from LC–MS raw data using MarkerLynx™ XS (version 4.1, Waters Co.). The data matrix was created with a method using the following parameters: retention time (t_R) 3.0–24.0 min, mass range *m/z* 100–900 Da, mass tolerance of 0.01 Da, and intensity threshold of 10 counts. The alignment of peaks across samples was performed within the range of ± 0.05 Da mass and ± 0.20 min t_R windows. For the parameters in t ApexTrack algorithm, the controls peak detection by peak width (peak width at 5% height) and baseline threshold (peak-to-peak baseline ratio) were automatically calculated by MarkerLynx. The noise elimination level was set to 50. As a result, 1471 ion markers were extracted from the twelve LC–MS profiles and arranged into a peak table (Supplementary Data). The preprocessed peak table data matrix was imported into SIMCA 13.0 (Umetrics, Umeå, Sweden) for multivariate analyses. The data matrix was normalized with Pareto-scaling method.

Acknowledgements

This research was supported by the Basic Science Research Program through the National Research Foundation of Korea (NRF), which was funded by the Ministry of Science, ICT and Future Planning (NRF-2015M3A9A5030733).

Appendix A. Supplementary data

Supplementary data related to this article can be found at https://doi.org/10.1016/j.phytochem.2018.07.012.

References

Aimi, N., Seki, H., Sakai, S., Haginiwa, J., 1993. Kinginoside, a new acyl group carrying iridoid bioside from *Lonicera morrowii*. Chem. Pharm. Bull. 41, 1882–1884.
Allen, G.C., Flores-Vergara, M.A., Krasnyanski, S., Kumar, S., Thompson, W.F., 2006. A modified protocol for rapid DNA isolation from plant tissues using cetyl-trimethylammonium bromide. Nat. Protoc. 1, 2320–2325.
Altschul, S.F., Gish, W., Miller, W., Myers, E.W., Lipman, D.J., 1990. Basic local alignment search tool. J. Mol. Biol. 215, 403–410.
Calis, I., Lahloub, M.F., Sticher, O., 1984. Loganin, loganic acid and periclymenoside, a new biosidic ester iridoid glucoside from *Lonicera periclymenum* L. (Caprifoliaceae). Helv. Chim. Acta 67, 160–165.
Chen, J., Xu, Y., Wei, G., Liao, S., Zhang, Y., Huang, W., Yuan, L., Wang, Y., 2015. Chemotypic and genetic diversity in *Epimedium sagittatum* from different geographical regions of China. Phytochemistry 116, 180–187.
Chen, J., Xia, N., Wang, X., Beeson Jr., R.C., Chen, J., 2017. Ploidy level, karyotype, and DNA content in the genus *Lonicera*. Hortscience 52, 1680–1686.
Choi, C.W., Jung, H.A., Kang, S.S., Choi, J.S., 2007. Antioxidant constituents and a new triterpenoid glycoside from Flos Lonicerae. Arch Pharm. Res. 30, 1–7.
Cipollini, D., Stevenson, R., Cipollini, K., 2008a. Contrasting direct and indirect effects of allelochemicals from two invasive plants on the performance of a non-mycorrhizal plant. Int. J. Plant Sci. 169, 371–375.
Cipollini, D., Dorning, M., 2008. Direct and indirect effects of conditioned soils and tissue extracts of the invasive shrub, *Lonicera maackii*, on target plant performance. Castanea 73, 166–176.
Cipollini, D., Stevenson, R., Enright, S., Eyles, A., Bonello, P., 2008b. Phenolic metabolites in leaves of the invasive shrub, *Lonicera maackii*, and their potential phytotoxic and anti-herbivore effects. J. Chem. Ecol. 34, 144–152.
de Bernonville, T.D., Foureau, E., Parage, C., Lanoue, A., Clastre, M., Londono, M.A., Oudin, A., Houille, B., Papon, N., Besseau, S., Glevarec, G., Atehortua, L., Giglioli-Guivarc'h, N., St-Pierre, B., De Luca, V., O'Connor, S.E., Courdavault, V., 2015. Characterization of a second secologanin synthase isoform producing both secologanin and secoxyloganin allows enhanced de novo assembly of a *Catharanthus roseus* transcriptome. BMC Genom. 16, 619.
Ding, Y., Cao, Z., Cao, L., Ding, G., Wang, Z., Xiao, W., 2017. Antiviral activity of chlorogenic acid against influenza A (H1N1/H3N2) virus and its inhibition of neuraminidase. Sci. Rep. 7, 45723.
Dobler, S., Petschenka, G., Pankoke, H., 2011. Coping with toxic plant compounds – the insect's perspective on iridoid glycosides and cardenolides. Phytochemistry 72, 1593–1604.
Es-Safi, N.E., Kerhoas, L., Ducrot, P.H., 2007. Fragmentation study of iridoid glucosides through positive and negative electrospray ionization, collision-induced dissociation and tandem mass spectrometry. Rapid Commun. Mass Spectrom. 21, 1165–1175.
Fabre, N., Rustan, I., de Hoffmann, E., Quetin-Leclercq, J., 2001. Determination of flavone, flavonol, and flavanone aglycones by negative ion liquid chromatography electrospray ion trap mass spectrometry. J. Am. Soc. Mass Spectrom. 12, 707–715.
Gao, Z.T., Liu, Y., Wang, X.Y., Song, J.Y., Chen, S.L., Ragupathy, S., Han, J.P., Newmaster, S.G., 2017. Derivative technology of DNA barcoding (nucleotide signature and SNP double peak methods) detects adulterants and substitution in Chinese patent medicines. Sci. Rep. 7, 5858.
Hamilton, J.G., Zangerl, A.R., DeLucia, E.H., Berenbaum, M.R., 2001. The carbon-nutrient balance hypothesis: its rise and fall. Ecol. Lett. 4, 86–95.
Hara, H., 1983. A Revision of Caprifoliaceae of Japan with Reference to Allied Plants in Other Districts and the Adoxaceae. Academia Scientific Book, Tokyo.
Hsu, P., Wang, H., 1988. Lonicera. In: Hsu, P., H. W., Hu, J. (Eds.), Flora Republicae Popularis Sinicae. Science Press, Beijing, pp. 153–257.
Irmler, S., Schroder, G., St-Pierre, B., Crouch, N.P., Hotze, M., Schmidt, J., Strack, D., Matern, U., Schroder, J., 2000. Indole alkaloid biosynthesis in *Catharanthus roseus*: new enzyme activities and identification of cytochrome P450CYP72A1 as secologanin synthase. Plant J. 24, 797–804.
Jaiswal, R., Muller, H., Muller, A., Karar, M.G., Kuhnert, N., 2014. Identification and characterization of chlorogenic acids, chlorogenic acid glycosides and flavonoids from *Lonicera henryi* L. (Caprifoliaceae) leaves by LC-MS^n. Phytochemistry 108, 252–263.
Kang, K.B., Lee, D.Y., Kim, M.S., Kim, T.B., Yang, T.J., Sung, S.H., 2018. Argininosecologanin, a secoiridoid-derived guanidine alkaloid from the roots of *Lonicera insularis*. Nat. Prod. Res. 32, 788–794.
Kim, K., Lee, S.C., Lee, J., Yu, Y., Yang, K., Choi, B.S., Koh, H.J., Waminal, N.E., Choi, H.I., Kim, N.H., Jang, W., Park, H.S., Lee, J., Lee, H.O., Joh, H.J., Lee, H.J., Park, J.Y., Perumal, S., Jayakodi, M., Lee, Y.S., Kim, B., Copetti, D., Kim, S., Kim, S., Lim, K.B., Kim, Y.D., Lee, J., Cho, K.S., Park, B.S., Wing, R.A., Yang, T.J., 2015. Complete chloroplast and ribosomal sequences for 30 accessions elucidate evolution of *Oryza* AA genome species. Sci. Rep. 5, 15655.
Kim, K., Nguyen, V.B., Dong, J.Z., Wang, Y., Park, J.Y., Lee, S.C., Yang, T.J., 2017. Evolution of the Araliaceae family inferred from complete chloroplast genomes and 45S nrDNAs of 10 *Panax*-related species. Sci. Rep. 7, 4917.
Kucharska, A.Z., Fecka, I., 2016. Identification of iridoids in edible honeysuckle berries (*Lonicera caerulea* L. var. *kamtschatica* Sevast.) by UPLC-ESI-qTOF-MS/MS. Molecules 21, 1157.
Kucharska, A.Z., Sokol-Letowska, A., Oszmianski, J., Piorecki, N., Fecka, I., 2017. Iridoids, phenolic compounds and antioxidant activity of edible honeysuckle berries (*Lonicera caerulea* var. *kamtschatica* Sevast.). Molecules 22, 405.
Lee, S.J., Shin, E.J., Son, K.H., Chang, H.W., Kang, S.S., Kim, H.P., 1995. Antiinflammatory activity of the major constituents of *Lonicera japonica*. Arch Pharm. Res. 18, 133–135.
Liu, Y., Wang, Y., Guo, F.X., Zhan, L., Mohr, T., Cheng, P., Huo, N.X., Gu, R.H., Pei, D.N., Sun, J.Q., Tang, L., Long, C.L., Huang, L.Q., Gu, Y.Q., 2017. Deep sequencing and transcriptome analyses to identify genes involved in secoiridoid biosynthesis in the Tibetan medicinal plant *Swertia mussotii*. Sci. Rep. 7, 43108.
March, R.E., Lewars, E.G., Stadey, C.J., Miao, X.S., Zhao, X.M., Metcalfe, C.D., 2006. A comparison of flavonoid glycosides by electrospray tandem mass spectrometry. Int. J. Mass Spectrom. 248, 61–85.
Naugzemys, D., Zilinskaite, S., Skridaila, A., Zvingila, D., 2014. Phylogenetic analysis of the polymorphic 4× species complex *Lonicera caerulea* (Caprifoliaceae) using RAPD markers and noncoding chloroplast DNA sequences. Biologia 69, 585–593.
Peñuelas, J., Sardans, J., Stefanescu, C., Parella, T., Filella, I., 2006. *Lonicera implexa* leaves bearing naturally laid eggs of the specialist herbivore *Euphydryas aurinia* have dramatically greater concentrations of iridoid glycosides than other leaves. J. Chem. Ecol. 32, 1925–1933.
Plumb, R.S., Johnson, K.A., Rainville, P., Smith, B.W., Wilson, I.D., Castro-Perez, J.M., Nicholson, J.K., 2006. UPLC/MS^E; a new approach for generating molecular fragment information for biomarker structure elucidation. Rapid Commun. Mass Spectrom. 20, 1989–1994.
Qi, L.W., Chen, C.Y., Li, P., 2009. Structural characterization and identification of iridoid glycosides, saponins, phenolic acids and flavonoids in Flos Lonicerae Japonicae by a fast liquid chromatography method with diode-array detection and time-of-flight mass spectrometry. Rapid Commun. Mass Spectrom. 23, 3227–3242.
Rai, A., Kamochi, H., Suzuki, H., Nakamura, M., Takahashi, H., Hatada, T., Saito, K., Yamazaki, M., 2017. De novo transcriptome assembly and characterization of nine tissues of *Lonicera japonica* to identify potential candidate genes involved in chlorogenic acid, luteolosides, and secoiridoid biosynthesis pathways. J. Nat. Med. 71, 1–15.
Rehder, A., 1903. Synopsis of the Genus Lonicera. Missouri Botanical Garden Annual Report, vol. 14 27–232.
Ren, M.T., Chen, J., Song, Y., Sheng, L.S., Li, P., Qi, L.W., 2008. Identification and quantification of 32 bioactive compounds in *Lonicera* species by high performance liquid chromatography coupled with time-of-flight mass spectrometry. J. Pharm. Biomed. Anal. 48, 1351–1360.
Schierenbeck, K.A., 2004. Japanese honeysuckle (*Lonicera japonica*) as an invasive

species; History, ecology, and context. Crit. Rev. Plant Sci. 23, 391–400.
Shang, X., Pan, H., Li, M., Miao, X., Ding, H., 2011. *Lonicera japonica* Thunb.: ethnopharmacology, phytochemistry and pharmacology of an important traditional Chinese medicine. J. Ethnopharmacol. 138, 1–21.
Smith, S.A., 2009. Taking into account phylogenetic and divergence-time uncertainty in a parametric biogeographical analysis of the Northern Hemisphere plant clade Caprifolieae. J. Biogeogr. 36, 2324–2337.
Smith, S.A., Donoghue, M.J., 2010. Combining historical biogeography with niche modeling in the Caprifolium clade of *Lonicera* (Caprifoliaceae, Dipsacales). Syst. Biol. 59, 322–341.
Sun, C., Teng, Y., Li, G., Yoshioka, S., Yokota, J., Miyamura, M., Fang, H., Zhang, Y., 2010. Metabonomics study of the protective effects of *Lonicera japonica* extract on acute liver injury in dimethylnitrosamine treated rats. J. Pharm. Biomed. Anal. 53, 98–102.
Tamura, K., Stecher, G., Peterson, D., Filipski, A., Kumar, S., 2013. MEGA6: molecular evolutionary genetics analysis version 6.0. Mol. Biol. Evol. 30, 2725–2729.
Theis, N., Donoghue, M.J., Li, J.H., 2008. Phylogenetics of the Caprifolieae and *Lonicera* (Dipsacales) based on nuclear and chloroplast DNA sequences. Syst. Bot. 33, 776–783.
Wang, L., Jiang, Q., Hu, J., Zhang, Y., Li, J., 2016. Research progress on chemical constituents of *Lonicerae japonicae flos*. BioMed Res. Int. 2016, 8968940.
Watling, J.I., Hickman, C.R., Lee, E., Wang, K., Orrock, J.L., 2011. Extracts of the invasive shrub *Lonicera maackii* increase mortality and alter behavior of amphibian larvae. Oecologia 165, 153–159.
Whitehead, S.R., Bowers, M.D., 2013. Iridoid and secoiridoid glycosides in a hybrid complex of bush honeysuckles (*Lonicera* spp., Caprifolicaceae): implications for evolutionary ecology and invasion biology. Phytochemistry 86, 57–63.
Wolfender, J.L., Marti, G., Thomas, A., Bertrand, S., 2015. Current approaches and challenges for the metabolite profiling of complex natural extracts. J. Chromatogr. A 1382, 136–164.
Yamamoto, H., Katano, N., Ooi, A., Inoue, K., 2000. Secologanin synthase which catalyzes the oxidative cleavage of loganin into secologanin is a cytochrome P450. Phytochemistry 53, 7–12.
Yamamoto, H., Katano, N., Ooi, Y., Inoue, K., 2000. Transformation of loganin and 7-deoxyloganin into secologanin by *Lonicera japonica* cell suspension cultures. Phytochemistry 50, 417–422.
Zhang, Y.D., Huang, X., Zhao, F.L., Tang, Y.L., Yin, L., 2015. Study on the chemical markers of Caulis *Lonicerae japonicae* for quality control by HPLC-QTOF/MS/MS and chromatographic fingerprints combined with chemometrics methods. Anal. Meth. 7, 2064–2076.